TU Delft

Delft University of Technology

Fully inkjet-printed dielectric elastomer actuators

Gallucci, Giulio; Wu, Yantong; Tichem, Marcel; Hunt, Andres

DOI
10.1117/12.3010872

Publication date
2024

Document Version
Final published version

Published in
Electroactive Polymer Actuators and Devices (EAPAD) XXVI

Citation (APA)
Gallucci, G., Wu, Y., Tichem, M., & Hunt, A. (2024). Fully inkjet-printed dielectric elastomer actuators. In J. D. Madden (Ed.), *Electroactive Polymer Actuators and Devices (EAPAD) XXVI* Article 129450I (Proceedings of SPIE - The International Society for Optical Engineering; Vol. 12945). SPIE. https://doi.org/10.1117/12.3010872

Important note
To cite this publication, please use the final published version (if applicable).
Please check the document version above.

Copyright
Other than for strictly personal use, it is not permitted to download, forward or distribute the text or part of it, without the consent of the author(s) and/or copyright holder(s), unless the work is under an open content license such as Creative Commons.

Takedown policy
Please contact us and provide details if you believe this document breaches copyrights.
We will remove access to the work immediately and investigate your claim.

This work is downloaded from Delft University of Technology.
For technical reasons the number of authors shown on this cover page is limited to a maximum of 10.

Fully inkjet-printed dielectric elastomer actuators

Giulio Gallucci, Yantong Wu, Marcel Tichem, and Andres Hunt

Department of Precision and Microsystems Engineering, Delft University of Technology, Mekelweg 2, 2628CD Delft, The Netherlands

ABSTRACT

Dielectric elastomers (DEs) have received significant attention for their good performance among different smart material transducers. This study demonstrates the feasibility of fabricating dielectric elastomer actuators (DEAs) using exclusively inkjet printing technique. The manufactured unimorph bending cantilevers are composed of a polydimethylsiloxane (PDMS) active layer, sandwiched between two compliant electrodes, and printed onto a thin polyimide (PI) substrate. This study addresses the key fabrication challenges associated with inkjet printing such a layered actuator structure. This entails the consistent printing of the Ag electrodes on the smooth PI substrate, a PDMS layer on the Ag electrodes, the Ag electrodes on the smooth PDMS surface, and the respective steps of processing and curing. The fully inkjet-printed DEAs exhibited a maximum tip displacement of 36 μm in quasi-static operation (1 kV_{pp}) and 12.8 μm in resonant operation (50 Hz, 800 V_{pp}). This is the first time that inkjet-printing has been employed to print an entire dielectric elastomer actuator, broadening the outlooks to develop innovative devices that base on smart material transducers.

Keywords: dielectric elastomer actuator, unimorph bending actuator, inkjet-printing, additive manufacturing, PDMS

1. INTRODUCTION

Among the diverse range of stimuli-responsive materials employed in soft actuator applications, dielectric elastomers, classified under electronic electroactive polymers (eEAPs),[1] have received considerable attention due to their promising electromechanical transduction characteristics. DEAs can be essentially described as compliant capacitors consisting of an elastomeric layer sandwiched between two thin electrodes. Application of a relatively high activation voltage ($\geqslant$ 1 kV)[2] across the electrodes induces electrostatic forces that compress the elastomer layer, causing lateral expansion. The resulting field-induced compressive stress σ, often denoted as Maxwell stress, is given by:[3] $\sigma = \varepsilon_0 \varepsilon_r \left(\frac{V}{\tau}\right)^2$, where ε_0 is the permittivity of free space, ε_r is the relative permittivity, V is the driving voltage, and τ is the film thickness. In the unimorph cantilever configuration (Figure 1a), the capacitor sandwich is laminated on a flexible passive layer. This additional mechanical constraint translates the in-plane lateral elongation of the elastomer into the bending motion of the entire structure.[4] Dielectric elastomer actuators (DEAs) are inherently lightweight and compliant, capable of demonstrating substantial strains and elastic energy densities of up to 380% and 3.4 J/cm^3, respectively.[5,6] DEAs have been explored as active components in soft robots,[7] microfluidic devices,[8–11] tactile displays,[12,13] deformable mirrors,[14] and isolation systems for suppression of vibrations.[15,16]

Additive manufacturing (AM) techniques are highly appealing for the versatile design and construction of functional transducers in various sizes and shapes, enabling more complex structuring (e.g., multilayered actuators) and reducing the labor intensity of the fabrication process. However, in the context of eEAP transducers production, AM methods are still in the early stages of development and present non-trivial challenges. These challenges encompass formulating printable inks,[17–19] obtaining pairs of conductive, electrically isolated compliant electrodes,[20–22] and achieving strong inter-layer adhesion.[23,24] Sikulskyi *et al.* developed a contact dispensing 3D printing process for bending unimorph DEAs (UDEAs).[18] The process is based on a Polydimethylsiloxane (PDMS) membrane with poly(3,4-ethylenedioxythiophene) polystyrene sulfonate (PEDOT:PSS) electrodes. Su *et al.* employed UV-cured extrusion to print acrylic elastomer films for multilayer DEAs.[17] In between each

Corresponding author: g.gallucci@tudelft.nl

Electroactive Polymer Actuators and Devices (EAPAD) XXVI, edited by John D. W. Madden, Proc. of SPIE Vol. 12945, 129450I
© 2024 SPIE · 0277-786X · doi: 10.1117/12.3010872

printing step, graphite electrodes were deposited by spray deposition with the aid of a mask. Araromi *et al.* recently reported a semi-automated spray deposition process for silicone-based multilayer UDEAs.[25] Koo *et al.* proposed a tactile cell stimulation design based on DEAs stacks.[26] They used spin-coating to deposit the elastomer film, and sprayed carbon powders to form the electrodes. The DEAs displacements reached 470 μm under 3.5 kV excitation at 0.1 Hz. A similar process was employed by Lotz *et al.* to fabricate DEAs stacks with thin (< 20 μm) PDMS layers.[27] The DEAs produced deformations of up to about 100 μm under driving voltages lower than 1 kV.

Fabricating complex geometries and thin layers of PDMS-based actuators at highest quality requires contactless and precise AM techniques. Drop on Demand (DoD) inkjet-printing (IJP) is such a technique that offers contactless, mask-free and fast thin film deposition, along with high versatility in terms of range of printable materials and transducer design.[19,28–30] IJP has been rarely investigated for DEAs fabrication and has been mainly employed to print DEAs electrodes. Chiolerio *et al.* IJP'ed PEDOT:PSS electrodes on plasma-modified PDSM nanocomposites designed for tactile sensing.[24] Shrestha *et al.* investigated optimal PEDOT:PSS ink composition for IJP transparent and uniform electrodes onto commercial acrylic elastomer membranes.[22] The IJP'ed electrodes exhibited electrical resistance in the range 1.15−5.54 kΩ. Yi *et al.* fabricated planar DEAs based on pre-stretched acrylic tape coated with IJP'ed carbon black (CB) electrodes.[31] The sheet resistance of the electrodes varied between 0.5 and 54 M$\Omega/\square$, depending on CB ink formulation and printing conditions. In a recent study, Mikkonen *et al.* demonstrated the fabrication of entirely IJP'ed multilayered circuit boards, consisting of thin Ag tracks isolated by a PDSM dielectric layer.[32] The printed conductive tracks exhibited notably low sheet resistance, below 0.3 $\Omega/\square$. However, when it comes to PDMS-based sensors and actuators, IJP of an entire functional transducer has not been reported.

This work develops a process for IJP functional PDMS-based dielectric elastomer actuators and experimentally characterizes their performance. The DEAs are based on the unimorph bending design shown in Figure 1b. The manufacturing process consists of three consecutive IJP steps for the Ag bottom electrode, PDMS active layer, and Ag top electrode, as detailed in (Section 2.1). The actuation performance is then characterized, as elaborated in Section 2.2. The work is concluded in Section 3.

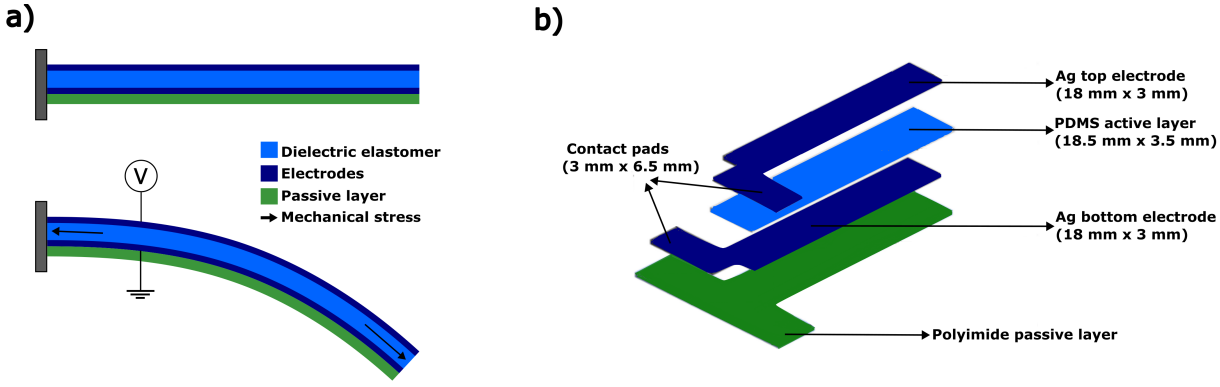

Figure 1: Unimorph bending DEAs: (a) working principle, and (b) the implemented design.

2. METHODOLOGY

2.1 Fabrication of unimorph DEAs

2.1.1 Bottom electrode

The bottom electrode is fabricated by jetting an Ag nanoparticle ink (NovaCentrix JS-A211, 40 wt.% Ag)[33] onto a 50 μm-thick polyimide passive layer using the Pixdro LP50 printer[34] (shown in Figure 2) and a DMC11610 printhead (16 nozzles, 21.5 μm orifice size, 245 μm nozzle pitch, 10 pL droplet volume).[35] To prevent unstable jetting and nozzle clogging due to Ag particles agglomeration, the JS-A211 ink is sonicated for 5 min and filtered with a 0.45 μm polytetrafluoroethylene (PTFE) filter before being loaded into the DMC11610 reservoir. The

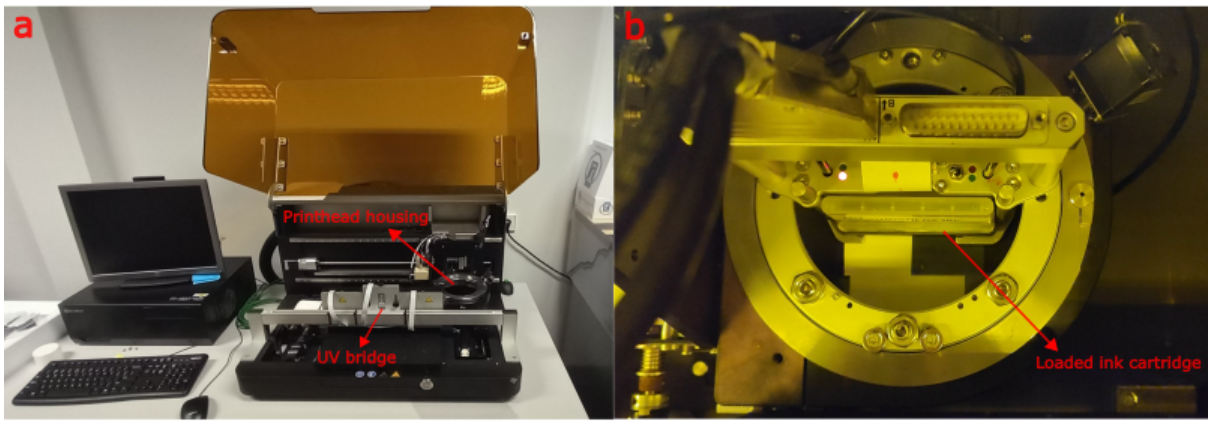

Figure 2: Inkjet-printing setup for fabricating the UDEAs: (a) the Pixdro LP50 inkjet printer platform, and (b) a close-up on the mounted printhead.

JS-A211 ink is jetted at a printing speed of 50.8 mm/s using 4 active nozzles firing at a 2 kHz frequency, yielding a printing resolution of 1000 DPI. During the printing the printbed temperature is maintained at 60 °C to speed up the solvent evaporation. In order to obtain a uniform and conductive film, two printing iterations are executed in succession. The as-deposited bottom electrode turns from a dark brown wet film into a shiny silver coating upon drying at 60 °C for 30 min.

To attain conductivity, it is essential to ensure proper densification of the deposited Ag nanoparticles.[19,36] The dried film is subjected to UV-sintering for 6 min at 1.2 W/cm^2 intensity with the continuous UV source (Phoseon FireEdge FE300) in the Pixdro LP50 system.[34] The wavelength of the UV source (345−385 nm) is close the plasmonic resonance absorption peak of the Ag nanoparticles in the JS-A211 ink,[19] which enable efficient sintering with exposures at lower intensities.[37] The resistance of the sintered electrodes, measured with a multimeter (Voltcraft VC820-1) from the contact pad to the beam tip (see Figure 1b), is of the order of 100 Ω.

2.1.2 PDMS layer

The base material used to formulate the PDMS ink is Sylgard-184, a bi-component elastomeric PDMS kit comprised of a polymeric base and a curing agent.[38] The base and the curing agent are mixed at a 10:1 ratio by mass, and octyl acetate (OA) is subsequently added for solvent, resulting in a PDMS concentration of 26 wt.%. The PDMS-OA mixture is sonicated for 15 min and filtered using a 1 μm PTFE filter before loading it in the DMC11610 reservoir. To ensure uniform coverage without the risk of nozzle clogging, the PDMS layer is printed using only one active nozzle at a 25.4 mm/s printing speed and 1 kHz firing frequency, resulting in a 1000 DPI resolution.

Since achieving electrical isolation between the two electrodes is crucial to obtain functional actuators, three printing iterations are performed. The printbed is maintained at 80°C to promote OA evaporation and crosslinking of PDMS during printing.[39] In between each iteration, the sample is left to cure on the heated printbed for 5 min to attain a semi-cured state, allowing better coverage of the next PDMS layer. This is also required to avoid overheating of the printhead above the printbed, which can safely withstand temperatures up to 60°C. Finally, the sample is treated in an oven (Memmert UN30) at 80°C for 3 hours to evaporate OA residuals and fully cure the elastomer.[40]

2.1.3 Top electrode deposition

After curing, the printed PDMS film surface is inherently hydrophobic.[41] Due to the aqueous nature of the JS-A211 Ag ink, the surface energy of PDMS needs to be lowered to achieve good wettability and strong adhesion with the top electrode. Surface activation of the cured samples is carried out by grafting functional polar groups with O_2 plasma treatment (Diener Femto) for 30 s at 40 W RF power. Increased RF power of the O_2 plasma (up to 100 W) resulted in a heavily damaged PDMS surface, with visible cracks spanning the whole length of the

beam. The surface functionalization introduced with O_2 plasma is not permanent, and a hydrophobic recovery occurs over time.[42] Therefore, the top electrode had to be printed within 3 hours post plasma treatment.

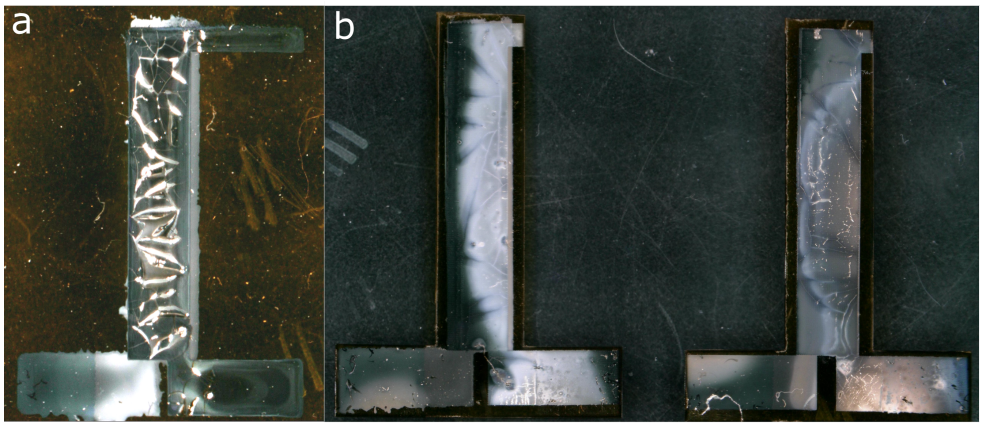

Figure 3: Inkjet-printed UDEAs: (a) cracks formation and delamination occurring on the Ag top electrode printed at a 1000 DPI resolution and dried at room temperature, and (b) laser-cut complete UDEAs with conductive top electrodes printed at 250 DPI resolution and dried at room temperature.

A major challenge in the deposition of thin nanoparticle films from colloidal suspensions is the formation of cracks and material delamination upon drying.[43–45] This is caused by the capillary forces arising in the particle network during solvent evaporation.[45] While no cracking occurred during the drying of the bottom electrode, the top electrode that was printed at identical settings formed visible cracks and material delamination (see Figure 3a) during drying, regardless of the drying temperature (20 °C, 40 °C and 60 °C were studied). This effect can be attributed to the different surface morphology and mechanical properties of the printed PDMS compared to the polyimide substrate.[46] Crack nucleation and propagation are known to occur during the drying of nanoparticle films with a thickness exceeding a critical value.[44,47]

To reduce the amount of deposited Ag and the final film thickness below critical, the printing of the top electrode is performed at a much lower resolution of 250 DPI (1 kHz frequency, 101.6 mm/s speed) than the other UDEA layers. Despite the lower resolution, full coverage of Ag on top of the PDMS surface can still be achieved due to the plasma-activated surface and the relatively large volume of the droplets ($\sim$ 10 pL). Both the printing (three iterations) and subsequent drying ($\sim$ 1 hour) processes are conducted at room temperature to mitigate the potential development of thermal stresses. Increased sintering durations and higher UV intensities are required compared to the bottom electrode since a very high level of particle coalescence is necessary to render the very thin Ag layer conductive. The measured resistances from the contact pad to the beam tip are of the order of 10 Ω upon 15 min of treatment at 3 W/cm^2 intensity. The main advantage of using UV over conventional thermal curing lies in the limited heating induced in the sample. This is crucial to prevent irreversible wrinkling and cracking due to the mismatch of thermal expansion coefficients of the UDEA constituent materials.[32] Eventually, the cantilever structure (Figure 3b) is released from the polyimde substrate using an Optec WS Starter laser micromachining system.

2.2 Actuation performance

Performance of the IJP'ed UDEAs was investigated by measuring their actuation in response to sinusoidal excitation and extracting their frequency responses upon incrementally increasing input voltages. These experiments were conducted on an experimental set-up shown in Figure 4a. A UDEA was vertically fixed to a 3D-printed clamp, making the the effects of gravity negligible (see Figure 4b). A conductive Ag paste (RS Pro 186-3600) was applied on the contact pads of the actuators to ensure good electrical connections to the clamp electrodes. The UDEAs were driven by a high voltage power amplifier (Smart Material HVA 1500-1/50), while simultaneously measuring their tip displacements with a laser triangulation sensor (Micro-Epsilon OptoNCDT 1900-10). The

experiments were controlled from a PC computer using the LabView 2018 software (National Instruments), via a USB-6211 data acquisition card (National Instruments). The block diagram of the experimental set-up is shown in Figure 4c.

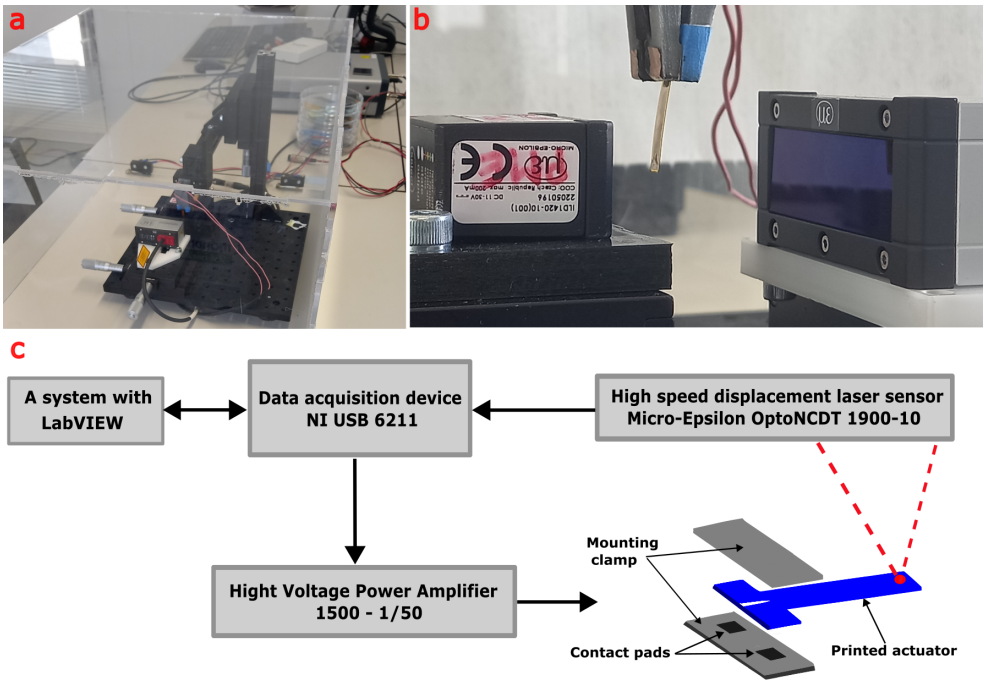

Figure 4: UDEAs performance characterization: (a) experimental set-up, (b) clamped actuator, (c) and schematic block diagram.

The frequency responses were measured upon unipolar sinusoidal excitation at 31 different frequencies, logarithmically distributed in the 0.1–100 Hz range. The input voltages were incrementally increased from 100 V_{pp} to 1 kV_{pp} with 100 V_{pp} increments. The resulting UDEAs frequency characteristic is plotted in Figure 5, indicating a resonant frequency of about 50 Hz. The largest resonant tip deflection of 12.8 μm was measured under 800 V_{pp} excitation while the largest resonant gain was attained at 300 V_{pp} excitation (1.85×10^{-5} mm/V, 5.5 μm amplitude).

Under quasi-static excitation (i.e. 0.1 Hz) the tip deflections of up to 36 μm were measured in response to 1 kV_{pp} excitation voltages. While the deflections increased with the voltage, a limited difference was observed in the actuation gain between the 200 V_{pp} and 700 V_{pp} excitation. This is caused by the viscoelastic behaviour of the polymer-based actuator , as indicated by the phase delays of the Bode plots (Figure 5) and actuation responses (Figure 6). Similarly, a decrease in the DEA deformation at higher excitation frequencies has been reported in multilayer DEAs,[27,48] and can be ascribed to the viscoelastic losses in the elastomer.[49]

The UDEAs remained completely functional at up to 900 V_{pp} inputs, and were operable at up to 1 kV_{pp} quasi-static excitation (see Figure 6b). At 1 kV_{pp} excitation, small sparks were observed on the top electrode surface as the driving frequency was increased, and the UDEAs' behaviour became inconsistent. The above maximum deflections are smaller than the 100 μm[27] and 470 μm[26] deformations reported for PDMS-based stack DEAs (driven under 0.6 and 3.5 kV inputs, respectively). It suggests that the performance of the fully inkjet-printed UDEAs' can be improved by increasing the volume of the active material by transferring from the single-layer UDEA design to multi-layer stacked actuators. This requires iterating the proposed IJP process to deposit additional PDMS-Ag layer combinations on top of the polyimide substrate.

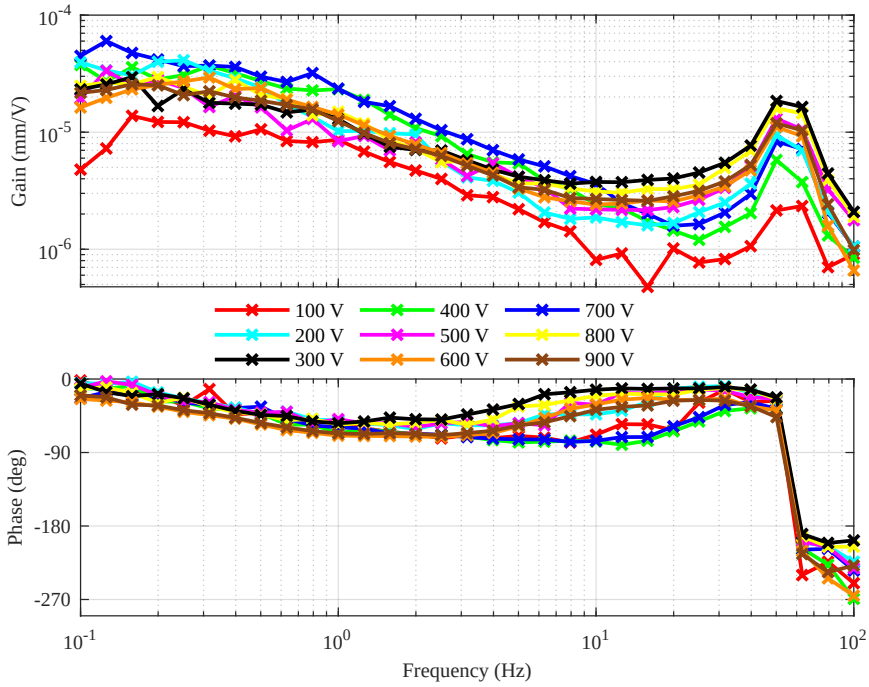

Figure 5: Frequency response of the IJP'ed UDEA at different input voltages.

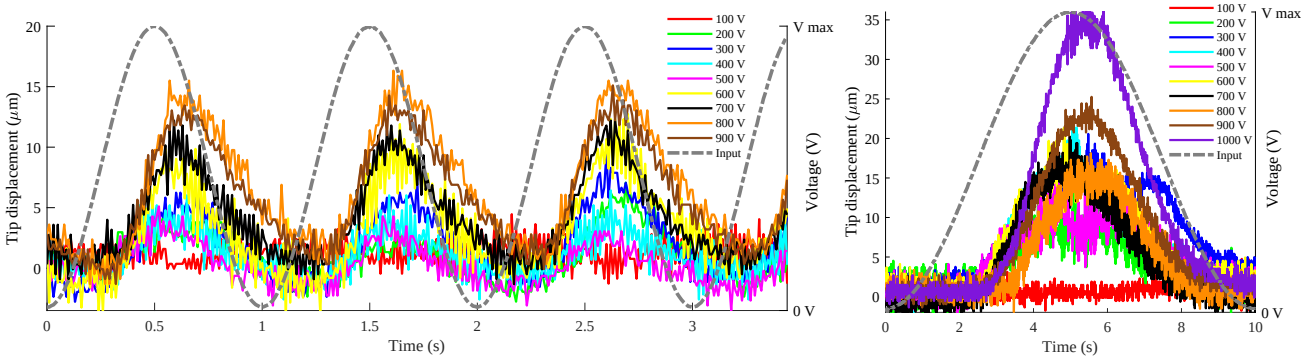

(a) (b)

Figure 6: UDEAs actuation in response to a sinusoidal excitation at 1 Hz (a) and 0.1 Hz (b).

3. CONCLUSIONS

In this work, an inkjet printing process was developed and implemented for fabricating entire bending cantilever actuators basing on PDSM elastomer and Ag electrodes. The resulting process enables contact-less additive manufacturing with minimum material wastage and can implement virtually arbitrary actuator designs with fine feature sizes. Challenges were addressed in depositing uniform films of PDMS elastomer and Ag electrodes, curing these material layers and attaining inter-layer adhesion. The manufactured actuators exhibited a maximum quasi-static tip displacement of 36 μm under 1 kV_{pp} excitation, and a maximum tip displacement at resonance (50 Hz, 800 V_{pp}) of 12.8 μm. The developed additive manufacturing process for PDMS-based UDEAs could be further extended for more complex designs and multilayer systems, enabling lower driving voltages and higher displacements. Being able to produce well-performing transducer of arbitrary geometry at the highest level of automation is essential for developing innovative devices that are functionalized by smart material transducers.

REFERENCES

[1] Bar-Cohen, Y., Cardoso, V., Ribeiro, C., and Lanceros-Méndez, S., "Chapter 8 - electroactive polymers as actuators," in [*Advanced Piezoelectric Materials (Second Edition)*], Uchino, K., ed., *Woodhead Publishing in Materials*, 319–352, Woodhead Publishing, second edition ed. (2017).

[2] Bar-Cohen, Y., "EAP as artificial muscles: progress and challenges," in [*Smart Structures and Materials 2004: Electroactive Polymer Actuators and Devices (EAPAD)*], Bar-Cohen, Y., ed., **5385**, 10–16, SPIE (2004).

[3] Suo, Z., "Theory of dielectric elastomers," *Acta Mechanica Solida Sinica* **23**(6), 549–578 (2010).

[4] Araromi, O. A. and Burgess, S. C., "A finite element approach for modelling multilayer unimorph dielectric elastomer actuators with inhomogeneous layer geometry," *Smart materials and structures* **21**(3), 032001 (2012).

[5] Brochu, P. and Pei, Q., "Advances in dielectric elastomers for actuators and artificial muscles," *Macromolecular Rapid Communications* **31**(1), 10–36 (2010).

[6] Pelrine, R., Kornbluh, R., Joseph, J., Heydt, R., Pei, Q., and Chiba, S., "High-field deformation of elastomeric dielectrics for actuators," *Materials Science and Engineering: C* **11**(2), 89–100 (2000).

[7] Youn, J.-H., Jeong, S. M., Hwang, G., Kim, H., Hyeon, K., Park, J., and Kyung, K.-U., "Dielectric elastomer actuator for soft robotics applications and challenges," *Applied Sciences* **10**(2) (2020).

[8] Maffli, L., Rosset, S., and Shea, H. R., "Mm-size bistable zipping dielectric elastomer actuators for integrated microfluidics," in [*Electroactive Polymer Actuators and Devices (EAPAD) 2013*], Bar-Cohen, Y., ed., **8687**, 86872M, SPIE (2013).

[9] McCoul, D., Murray, C., Carlo, D. D., and Pei, Q., "Dielectric elastomer actuators for active microfluidic control," in [*Electroactive Polymer Actuators and Devices (EAPAD) 2013*], Bar-Cohen, Y., ed., **8687**, 86872G, SPIE (2013).

[10] Murray, C., McCoul, D., Sollier, E., Ruggiero, T., Niu, X., Pei, Q., and Carlo, D. D., "Electro-adaptive microfluidics for active tuning of channel geometry using polymer actuators," *Microfluidics and nanofluidics* **14**, 345–358 (2013).

[11] Loverich, J. J., Kanno, I., and Kotera, H., "Concepts for a new class of all-polymer micropumps," *Lab Chip* **6**, 1147–1154 (2006).

[12] Vishniakou, S., Lewis, B. W., Niu, X., Kargar, A., Sun, K., Kalajian, M., Park, N., Yang, M., Jing, Y., Brochu, P., et al., "Tactile feedback display with spatial and temporal resolutions," *Scientific reports* **3**(1), 2521 (2013).

[13] Kim, U., Kang, J., Lee, C., Kwon, H. Y., Hwang, S., Moon, H., Koo, J. C., Nam, J.-D., Hong, B. H., Choi, J.-B., and Choi, H. R., "A transparent and stretchable graphene-based actuator for tactile display," *Nanotechnology* **24**(14), 145501 (2013).

[14] Kornbluh, R., Flamm, D., Prahlad, H., Nashold, K., Chhokar, S., Pelrine, R., Huestis, D., Simons, J., Cooper, T., and Watters, D., "Shape control of large lightweight mirrors with dielectric elastomer actuation," *Proceedings of SPIE - The International Society for Optical Engineering* **5051**, 143 – 158 (2003).

[15] Karsten, R., Flittner, K., Haus, H., and Schlaak, H. F., "Development of an active isolation mat based on dielectric elastomer stack actuators for mechanical vibration cancellation," in [*Electroactive Polymer Actuators and Devices (EAPAD) 2013*], **8687**, 295–302, SPIE (2013).

[16] Graf, C. and Maas, J., "Electroactive polymer devices for active vibration damping," in [*Electroactive Polymer Actuators and Devices (EAPAD) 2011*], Bar-Cohen, Y. and Carpi, F., eds., **7976**, 79762I, SPIE (2011).

[17] Su, S., He, T., and Yang, H., "3d printed multilayer dielectric elastomer actuators," *Smart Materials and Structures* **32**(3), 035021 (2023).

[18] Sikulskyi, S., Ren, Z., Mekonnen, D. T., Holyoak, A., Srinivasaraghavan Govindarajan, R., and Kim, D., "Additively manufactured unimorph dielectric elastomer actuators: Design, materials, and fabrication," *Frontiers in Robotics and AI* **9** (2022).

[19] Sekar, S. and Hunt, A., "Inkjet printing p (vdf-trfe-ctfe) actuators for large bending strains," *Smart Materials and Structures* **33**(2), 025036 (2024).

[20] Lau, G.-K., Goh, S. C.-K., and Shiau, L.-L., "Dielectric elastomer unimorph using flexible electrodes of electrolessly deposited (eld) silver," *Sensors and Actuators A: Physical* **169**(1), 234–241 (2011).

[21] IJssel de Schepper, S. and Hunt, A., "An airbrush 3d printer: Additive manufacturing of relaxor ferroelectric actuators," *Additive Manufacturing* **81**, 103982 (2024).

[22] Shrestha, M., Lu, Z., and Lau, G.-K., "Transparent tunable acoustic absorber membrane using inkjet-printed pedot:pss thin-film compliant electrodes," *ACS Applied Materials & Interfaces* **10**(46), 39942–39951 (2018).

[23] Guo, Y., Liu, L., Liu, Y., and Leng, J., "Review of dielectric elastomer actuators and their applications in soft robots," *Advanced Intelligent Systems* **3**(10), 2000282 (2021).

[24] Chiolerio, A., Rivolo, P., Porro, S., Stassi, S., Ricciardi, S., Mandracci, P., Canavese, G., Bejtka, K., and Pirri, C. F., "Inkjet-printed pedot: Pss electrodes on plasma-modified pdms nanocomposites: Quantifying plasma treatment hardness," *Rsc Advances* **4**(93), 51477–51485 (2014).

[25] Araromi, O., Conn, A., Ling, C., Rossiter, J., Vaidyanathan, R., and Burgess, S., "Spray deposited multilayered dielectric elastomer actuators," *Sensors and Actuators A: Physical* **167**(2), 459–467 (2011). Solid-State Sensors, Actuators and Microsystems Workshop.

[26] Koo, I. M., Jung, K., Koo, J. C., Nam, J.-D., Lee, Y. K., and Choi, H. R., "Development of soft-actuator-based wearable tactile display," *IEEE Transactions on Robotics* **24**(3), 549–558 (2008).

[27] Lotz, P., Matysek, M., and Schlaak, H. F., "Fabrication and application of miniaturized dielectric elastomer stack actuators," *IEEE/ASME Transactions on Mechatronics* **16**(1), 58–66 (2011).

[28] Lu, G.-S., You, P.-C., Lin, K.-L., Hong, C.-C., and Liou, T.-M., "Fabricating high-resolution offset color-filter black matrix by integrating heterostructured substrate with inkjet printing," *Journal of Micromechanics and Microengineering* **24**(5), 055008 (2014).

[29] Ko, S. H., Pan, H., Grigoropoulos, C. P., Luscombe, C. K., Fréchet, J. M., and Poulikakos, D., "All-inkjet-printed flexible electronics fabrication on a polymer substrate by low-temperature high-resolution selective laser sintering of metal nanoparticles," *Nanotechnology* **18**(34), 345202 (2007).

[30] Bevione, M. and Chiolerio, A., "Benchmarking of inkjet printing methods for combined throughput and performance," *Advanced Engineering Materials* **22**(12), 2000679 (2020).

[31] Yi, J., Babick, F., Strobel, C., Rosset, S., Ciarella, L., Borin, D., Wilson, K., Anderson, I., Richter, A., and Henke, E.-F. M., "Characterizations and inkjet printing of carbon black electrodes for dielectric elastomer actuators," *ACS Applied Materials & Interfaces* **15**(35), 41992–42003 (2023).

[32] Mikkonen, R., Puistola, P., Jönkkäri, I., and Mäntysalo, M., "Inkjet printable polydimethylsiloxane for all-inkjet-printed multilayered soft electrical applications," *ACS Applied Materials & Interfaces* **12**(10), 11990–11997 (2020).

[33] "Novacentrix 2020 Metalon JS-A211 nanosilver ink - aqueous dispersion for inkjet printing (NCC Nano LLC)." Available at: https://www.novacentrix.com/datasheet/Metalon-JS-A211-TDS.pdf. (Accessed: 15 Febraury 2024).

[34] "Pixdro LP50 - SUSS MicroTec Specifications." Available at: https://www.suss.com/en/products-solutions/inkjet-printing/lp50. (Accessed: 15 Febraury 2024).

[35] Yoshinori, K., "FUJIFILM Group's inkjet printhead and technology." Available at: https://www.ekkotech.com/file/Fuji%20Group%20Printhead%20&%20Technology.pdf. (Accessed: 15 Febraury 2024).

[36] Corsino, D. C. and Balela, M. D. L., "Room temperature sintering of printer silver nanoparticle conductive ink," in [*IOP Conference Series: Materials Science and Engineering*], **264**(1), 012020, IOP Publishing (2017).

[37] Rajan, K., Roppolo, I., Chiappone, A., Bocchini, S., Perrone, D., and Chiolerio, A., "Silver nanoparticle ink technology: state of the art," *Nanotechnology, science and applications* , 1–13 (2016).

[38] "SYLGARD 184 Silicone Elastomer Kit." Available at: https://www.dow.com/en-us/pdp.sylgard-184-silicone-elastomer-kit.01064291z.html#overview. (Accessed: 15 Febraury 2024).

[39] Wang, Z., Volinsky, A. A., and Gallant, N. D., "Crosslinking effect on polydimethylsiloxane elastic modulus measured by custom-built compression instrument," *Journal of Applied Polymer Science* **131**(22) (2014).

[40] Prabowo, F., Wing-Keung, A. L., and Shen, H. H., "Effect of curing temperature and cross-linker to pre-polymer ratio on the viscoelastic properties of a pdms elastomer," in [*Advanced Materials Research and Production*], *Advanced Materials Research* **1112**, 410–413, Trans Tech Publications Ltd (8 2015).

[41] Mata, A., Fleischman, A. J., and Roy, S., "Characterization of polydimethylsiloxane (pdms) properties for biomedical micro/nanosystems," *Biomedical microdevices* **7**, 281–293 (2005).

[42] Bodas, D. and Khan-Malek, C., "Hydrophilization and hydrophobic recovery of pdms by oxygen plasma and chemical treatment—an sem investigation," *Sensors and Actuators B: Chemical* **123**(1), 368–373 (2007).

[43] Peng Xu, A. S. M. and Yu, B., "Drying-induced cracks in thin film fabricated from colloidal dispersions," *Drying Technology* **27**(5), 636–652 (2009).

[44] Carreras, E. S., Chabert, F., Dunstan, D., and Franks, G., "Avoiding "mud" cracks during drying of thin films from aqueous colloidal suspensions," *Journal of colloid and interface science* **313**(1), 160–168 (2007).

[45] Schneider, M., Maurath, J., Fischer, S. B., Weiß, M., Willenbacher, N., and Koos, E., "Suppressing crack formation in particulate systems by utilizing capillary forces," *ACS Applied Materials & Interfaces* **9**(12), 11095–11105 (2017).

[46] Smith, M. I. and Sharp, J. S., "Effects of substrate constraint on crack pattern formation in thin films of colloidal polystyrene particles," *Langmuir* **27**(13), 8009–8017 (2011).

[47] Prosser, J. H., Brugarolas, T., Lee, S., Nolte, A. J., and Lee, D., "Avoiding cracks in nanoparticle films," *Nano Letters* **12**(10), 5287–5291 (2012).

[48] Jia, K., Lu, T., and Wang, T., "Response time and dynamic range for a dielectric elastomer actuator," *Sensors and Actuators A: Physical* **239**, 8–17 (2016).

[49] Deguchi, S., Hotta, J., Yokoyama, S., and Matsui, T. S., "Viscoelastic and optical properties of four different pdms polymers," *Journal of Micromechanics and Microengineering* **25**(9), 097002 (2015).